2D MODELING OF MODERATOR FLOW AND TEMPERATURE DISTRIBUTION AROUND A SINGLE CHANNEL AFTER PRESSURE TUBE/CALANDRIA TUBE CONTACT

A. BEHDADI, J.C. LUXAT

McMaster University, Engineering Physics Department, Hamilton, Ontario, Canada L8S 4L7
e-mail: behdada@mcmaster.ca; luxatj@mcmaster.ca

ABSTRACT

A 2D computational fluid dynamics (CFD) model has been developed to calculate the moderator velocity field and temperature distribution around a single channel inside the moderator of a CANDU reactor after a postulated ballooning deformation of the pressure tube (PT) into contact with the calandria tube (CT). Following contact between the hot PT and the relatively cold CT, there is a spike in heat flux to the moderator surrounding the CT which may lead to sustained CT dryout. This can detrimentally affect channel integrity if the CT post-dryout temperature becomes sufficiently high to result in thermal creep strain deformation. The present research is focused on establishing the limits for dryout occurrence on the CTs for the situation in which pressure tube-calandria tube contact occurs. In order to consider different location of the channels inside the calandria, both upward and downward flow directions have been analyzed. The standard $k-\varepsilon$ turbulence model associated with logarithmic wall function is applied to predict the effects of turbulence. The governing equations are solved by the finite element software package COMSOL. The buoyancy driven natural convection on the outer surface of a CT has been analyzed to predict the flow and temperature distribution around the single CT considering the local moderator subcooling, wall temperature and heat flux. The model also shows the effect of high CT temperature on the flow and subcooling around the CTs at higher/lower elevation depending on the flow direction in the domain. According to the flow pattern and temperature distribution, it is predicted that stable film boiling generates in the stagnation region on the cylinder.

1. INTRODUCTION

In a CANDU reactor, the calandria is a horizontal cylindrical tank, filled by heavy water moderator circulated by a system of pumps at a rate of about $1m^3/s$. This vessel is 6 m long and its diameter is about 7.6 m (Figure 1).

There is a coaxial cylindrical core region inside the calandria shell with a smaller diameter of 6.3 m containing either 380 (CANDU-6) or 480 (Darlington/Bruce) fuel channels displacing about 10% of the total vessel volume. Each fuel channel consists of an outer calandria tube (CT) surrounding a coaxial pressure tube (PT) in which the heavy water coolant removes heat

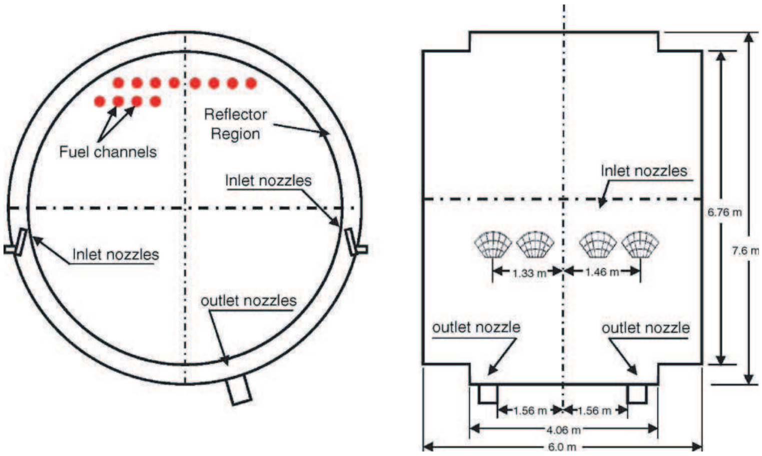

Figure 1. Calandria vessel[13]

from the fuel bundles. Four inlet nozzles are located at the middle of the left and right sidewall, pointing upward. The moderator fluid is discharged through two outlet nozzles at the bottom of the tank and cooled by the moderator heat exchangers before returning through the inlet nozzles. The inlet velocity is about 2 m/s and the outlet velocity is between 5 and 7 m/s. [11] The heat generation rate inside the moderator is up to 900 kW/m^3 in the fuel channel region and about 100 kW/m^3 in the reflector region. In these conditions the flow field is generally turbulent.[11]

In some loss of coolant accidents (LOCA), referred to as critical break LOCA, fuel cooling becomes severely degraded due to rapid flow reduction in the affected flow pass of the heat transport system. This can result in pressure tubes experiencing significant heatup while coolant pressure is still high, thereby causing uniform thermal creep strain (ballooning) of the PT into contact with its CT.[10] Contact of the hot PT with the CT leads to rapid redistribution of stored heat from the PT to CT and a large spike in heat flux from the CT to the moderator fluid. For lower subcooling conditions of the moderator, dryout of the CT can occur (Figure2).

Experimental studies on the flow and temperature distribution inside the moderator have been performed in Canada since the early 1980s. Austman et al., [8] measured the moderator temperature by inserting thermo-couples through a shut-off rod guide tube in operating CANDU reactors at Bruce A and Pickering. Huget et al., [15, 16] performed 2D moderator circulation tests at a 1/4-scaled facility in the Stern Laboratories in Canada. Three distinct flow patterns were observed from these studies, corresponding to different range of Archimedes number. Khartabil et al., [9] performed 3D moderator circulation tests in the moderator temperature facility (MTF) in the Chalk River Laboratories of Atomic Energy of Canada Limited. These tests had been conducted along with separate effect tests such as a hydraulic resistance through tube bundles, velocity profiles at an inlet diffuser, flow development along a curved wall and the turbulence generation by temperature differences.

Szymanski et. al, [11]developed a thermal-hydraulic code, called MODTURC, to calculate

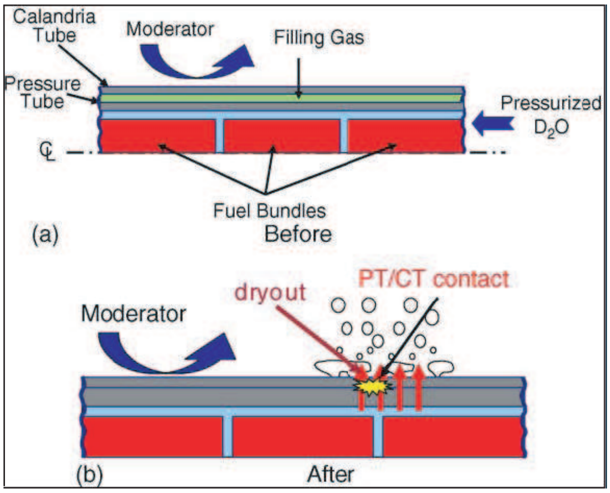

Figure 2. PT/CT contact phenomena: (a) before and (b) after [13]

the moderator temperature and velocity distribution in the calandria of a CANDU reactor. They used finite difference technique and $k - \varepsilon$ turbulence model to solve 3D equations. They also compared the code predictions to experimental results of one reactor design and found satisfactory agreement. Based on these works, a CFD (Computational Fluid Dynamics) code called MODTURC-CLAS (Moderator TURbulent Circulation Co-Located Advanced Solution) has been developed by Ontario Power Generation (OPG) and selected as Canadian Industry Standard Toolset (IST). On the other hand, the CFD models based on commercial codes have been developed for predicting a CANDU-6 moderator temperature. Yoon et al., [1–3] developed a CFD model with a porous media approach for the core region in order to predict the moderator circulation inside the calandria of CANDU reactor under normal operating conditions and LOCA transients, using CFX-4 code (ANSYS Inc.). Manwoong Kim et al.,[13] investigated the moderator thermalhydraulic characteristics using the FLUENT code. They modelled all the calandria tubes as heating pipes without any approximation for the core region and predicted three flow patterns inside the moderator , i.e., momentum dominated flow, buoyancy dominated flow and mixed type flow depending on the inlet flow rate, heat load, or both. The authors investigated the moderator thermalhydraulic characteristics using their optimized model and found that the fuel channel integrity can be assured, and no boiling occurs. They also found that since the moderator has enough coolability as the alternate heat sink, the flow pattern does not significantly change.

Obviously, these previous studies have been done for the whole calandria. It is a concern that when PT/CT contact occurs in a channel, local moderator boiling may leads to CT dryout and may affect the flow around the CTs at higher elevations. This can detrimentally affect channel integrity if the CT post-dryout temperature becomes sufficiently high to result in thermal creep strain deformation. According to the importance of local flow and temperature distribution for dryout predictions around a single channel, this study has been performed to investigate the above mentioned problem using the general purpose finite element code COMSOL.

2. MODEL DESCRIPTION

COMSOL, is used for the thermal-hydraulic analysis of the CANDU moderator circulation around one single channel in a transient condition after a postulated PT/CT contact. In such condition, a large amount of heat transfers to the moderator which could lead to sustained CT dryout. Since the accident could occur in different locations inside the moderator and the flow distribution depends on the position of the channel, two kinds of initial flow are considered i.e. upward flow and downward flow. Therefore, the differences in buoyancy effects for upward and downward flow can be taken into account.

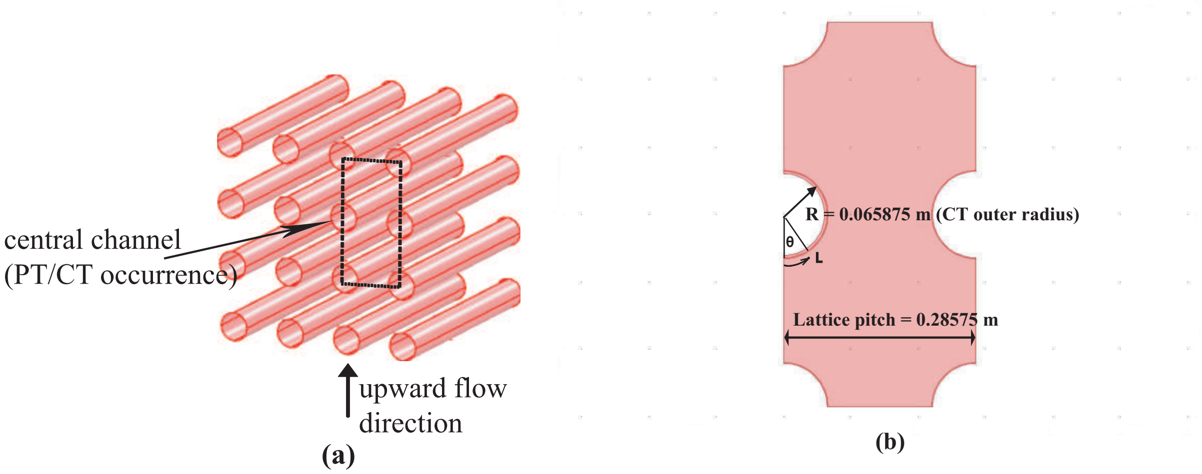

Figure 3. a) part of calandria tubes in 3D, b) the model geometry in 2D

2.1 ASSUMPTIONS AND GOVERNING EQUATIONS

In this model, a single phase fluid inside the moderator and a uniform PT/CT contact has been considered. The geometry is depicted in Figure 3-a. The arrow indicates the flow direction for upward flow. Neglecting any end effects from the walls of the vessel, the solution is constant in the direction of the tubes and therefore the model is reduced to a 2D domain. The dashed line marks the model region in 2D which is shown in the Figure 3-b. L is the arc-length associated with the angle θ on the surface of the central CT in which PT/CT contact occurrence is considered. Effect of neighboring channels on the flow field is taken into account by including part of them into the domain. Since the flow inside the moderator is turbulent the $k-\varepsilon$ turbulence model associated with logarithmic wall function is used. The governing equations in this model are:

- Reynolds Averaged Navier-Stokes (RANS) equations and a $k-\varepsilon$ turbulence model[5] in the heavy water moderator domain:

$$\frac{\partial \rho}{\partial t} + \nabla \cdot (\rho \mathbf{U}) = 0 \tag{1}$$

$$\rho\frac{\partial\mathbf{U}}{\partial t}+\rho\mathbf{U}\cdot\nabla\mathbf{U}=\nabla(-p+(\eta+\eta_T)(\nabla\mathbf{U}+(\nabla\mathbf{U})^T-\frac{2}{3}(\nabla\cdot\mathbf{U})\mathbf{I})-\frac{2}{3}\rho k\mathbf{I})+\mathbf{F} \quad (2)$$

$$\rho\frac{\partial k}{\partial t}-\nabla\cdot[(\eta+\frac{\eta_T}{\sigma_k})\nabla k]+\rho\mathbf{U}\cdot\nabla k=\frac{1}{2}\eta_T(\nabla\mathbf{U}+(\nabla\mathbf{U})^T)^2-\rho\varepsilon \quad (3)$$

$$\rho\frac{\partial\varepsilon}{\partial t}-\nabla\cdot[(\eta+\frac{\eta_T}{\sigma_\varepsilon})\nabla\varepsilon]+\rho\mathbf{U}\cdot\nabla\varepsilon=\frac{1}{2}C_{\varepsilon 1}\frac{\varepsilon}{k}\eta_T(\nabla\mathbf{U}+(\nabla\mathbf{U})^T)^2-\rho C_{\varepsilon 2}\frac{\varepsilon^2}{k} \quad (4)$$

- Heat transport equations in the water domain and the solid tube walls (CT thickness):

$$\rho C_p(\frac{\partial T}{\partial t}+\mathbf{U}\cdot\nabla T)+\nabla\cdot(-(\mathrm{k}+\mathrm{k}_T)\nabla T)=Q \quad (5)$$

Where,

$\mathbf{U}$ is average velocity field, $[m/s]$
$\mathbf{F}$ is body force, $[N/m^3]$
p is pressure, $[Pa]$
ρ is fluid density, $[kg/m^3]$
η is dynamic viscosity, $[Pa.s]$
∇ is vector differential operator
η_T is turbulent viscosity ($\rho C_p\frac{k^2}{\varepsilon}$), $[Pa.s]$
k is the turbulent kinetic energy, $[m^2/s^2]$
ε is the dissipation rate of turbulence energy, $[m^2/s^3]$
k is the fluid thermal conductivity, $[W/(m.K)]$
t is time, $[s]$
k_T is turbulence thermal conductivity($\frac{C_p\eta_T}{Pr_T}$), $[W/(m.K)]$
C_p is heat capacity, $[J/(kg.K)]$
Pr_T is turbulent Prandtl number

The model constants in the above equations are determined from experimental data[5]; their values are: C_μ= 0.09, $C_{\varepsilon 1}$= 1.44, $C_{\varepsilon 2}$= 1.92, σ_k= 1.0, σ_ε= 1.3. The $k-\varepsilon$ turbulence model, relies on several assumptions, the most important of which are that the Reynolds number is high enough and the turbulence is in equilibrium in boundary layers, which means that production equals dissipation.

The above equations are solved simultaneously inside the domain shown in Figure3-b using finite element method[14] in order to find the unknowns $(\mathbf{U}(\mathbf{u},\mathbf{v}),p,T,k,\varepsilon)$. The number of elements is 6230 with unstructured mesh as an optimized numbers in accordance with the mesh sensitivity analysis describing in section 2.3. Number of degree of freedom is 58062. Physical properties of water as a function of temperature are implemented from XSteam into the model[7]. Material properties of zircaloy as a function of temperature are taken from the ZRPRO [12].

2.2 BOUNDARY CONDITIONS

Two groups of boundary conditions are applied to the model, one group is for the $k-\varepsilon$ equations 1 to 4 in the fluid domain and the other group is for the heat transport equation 5.

For $k-\varepsilon$ equations in the fluid domain, a pressure difference between inlet and outlet given by the mass flow is applied. At the inlet and outlet normal flow and stream-wise periodic conditions for velocity, U, turbulent kinetic energy, k, and turbulent dissipation rate, ε are considered. The region borders are considered to be symmetric and at the CTs surfaces a logarithmic wall function is implemented. Basically two approaches can be used for solid walls in turbulent flow. In the first approach the equations are modified by additional terms and factors in order to consider the near wall effects and the mesh size near the wall must be fine enough to resolve the viscous sublayer. Such methods are of interest for moderate Reynolds numbers, where near wall resolution leads to a reasonable number of elements . In the second approach which is used in this study a constitutive relation between the velocity and surface shear stress replaces the thin boundary layer near the wall[5]. These relations known as wall functions are accurate for high Reynolds numbers and situations where pressure variations are not very large along the wall. In this approach it is assumed that the computational domain begins a distance δ_W from the actual wall and the flow is parallel to the wall[4].

For the heat transport equation, moderator temperature with different subcoolings at the inlet and convection dominated transport at the outlet of the domain are applied. At the inner surface of calandria tubes a heat flux associated with normal operation is implemented. While, in central one after a postulated PT/CT contact, the applied heat flux is drastically increased with time until the saturation point is reached in the fluid. The borders of the domain are considered to be symmetric. In order to model the temperature in the laminar sublayer at the CT/liquid interface, a thermal wall function (equation 6) is applied which relates the resistance to heat transfer through the laminar sublayer to that for momentum transfer for the fluid. The heat flux is determined by:[4]

$$q = \frac{\rho C_p C_\mu^{0.25} k_w^{0.5} (T_w - T)}{T^+} \tag{6}$$

where, ρ and C_p are the fluid density and heat capacity, respectively, C_μ is a numerical constant of the turbulence model, and k_w is the turbulent kinematic energy at the wall. Furthermore, T_w is the wall temperature while T is the fluid temperature. The quantity T^+ is related to the wall offset in viscous units, δ_w^+, through the definition:

$$T^+ = \frac{Pr_T}{\kappa} ln(\delta_w^+) + \beta \tag{7}$$

where the turbulent Prandtl number Pr_T is fixed to 0.85[17], the von Karman constant κ is set to 0.41 and β is a model constant set to 3.27. The wall offset in viscous units is defined as:

$$\delta_w^+ = \frac{\delta_w C_\mu^{0.25} k_w^{0.5}}{\nu} \tag{8}$$

where, δ_w is specified wall offset which is considered as half the local mesh size at the boundary and $\nu = \eta/\rho$ is the kinematic viscosity.

2.3 MESH EFFECT

The fluid velocity, the heat transfer coefficient and consequently the temperature at the boundaries are very sensitive to the number of mesh. The logarithmic wall function in section 2.2 is valid under certain conditions that depend on the resolution, the velocity and the viscosity. The wall function uses the dimensionless wall offset which for the first internal node should be less than some upper limit dependent on the Reynolds number.

Figure 4 depicts the wall offset parameter versus the CT surface arc-length for various subcoolings. Referring to the Figure 3- b, zero arc-length indicates the arc-length of the lowest point of the cylinder in the geometry ($\theta = 0°$) and arc-length equal to 0.21 indicates the top of the cylinder ($\theta = 180°$). Since the logarithmic wall functions are formally valid for δ_w^+ between 30 and 100[4] the number of mesh at the boundary has been made fine enough to satisfy this condition and to get accurate fluid velocity and heat transfer coefficient at the CT surface. Eventually, maximum applied mesh size on the central CT surface is about 1mm.

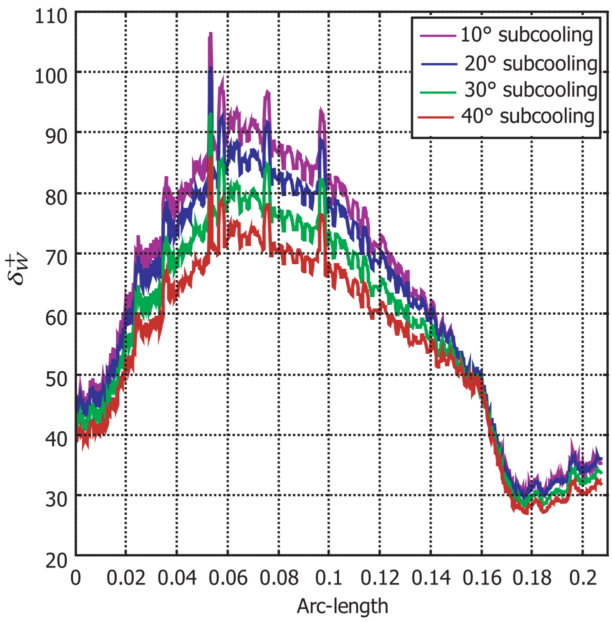

Figure 4. Wall offset in viscous units at the CT surface for various subcoolings

3. RESULTS AND DISCUSSION

The main objective of this study is to determine the nature of the temperature fluctuations and the interplay of velocity and temperature field in the vicinity of the calandria tubes after PT/CT contact. The model considers the steady state solution as initial value for the transient condition. The following Figures show the conditions around the central CT (see Figure 3) at 1second after PT/CT contact.

Figure 5 shows the local pressure and velocity variations in the condition that fluid enters the domain from the bottom with $0.5m/s$ velocity and $20°C$ subcooling. In this condition the Reynolds number is around 65000. The Figure indicates the opposite behavior of velocity and pressure on the cylinder. From $U = 0$ at the stagnation point ($\theta = 0$), the fluid accelerates due to the pressure gradient ($dU/dL > 0$ when $dp/dL < 0$), reaches to a maximum velocity when $dp/dL = 0$ (L denotes the arc-length) and decelerates as a result of the adverse pressure gradient ($dU/dL < 0$ when $dp/dL > 0$). Eventually the sign of velocity gradients changes and velocity becomes zero at the separation point where the boundary layer detaches from the surface and a wake is formed in the downstream region (see Figure6). The flow behavior is in very good agreement with the flow profile normal to circular cylinder described by Incropera[6].

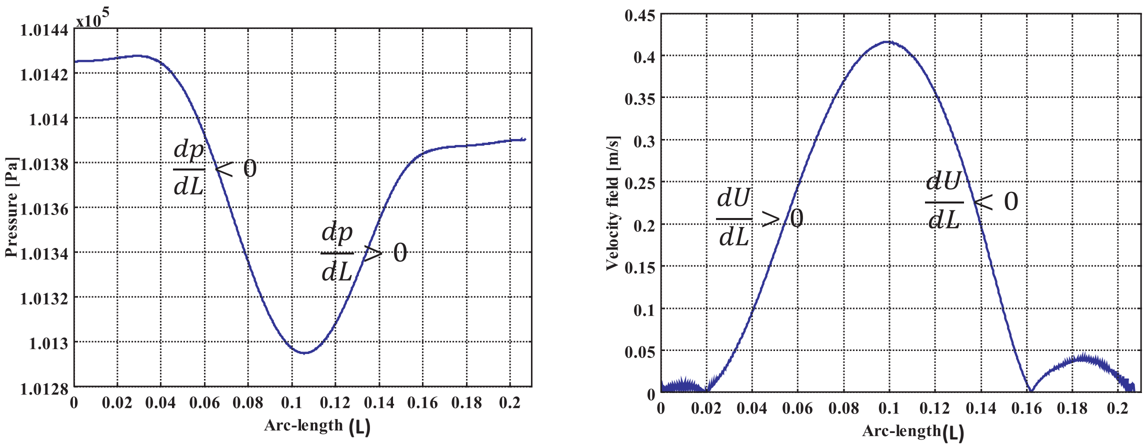

(a) (b)

Figure 5. (a) Local pressure (b) Local velocity

Figure6 shows the recirculation zones in the wake region behind the tube and also the stagnation point for an inlet flow velocity of $0.5m/s$ for both upward and downward flow. Arrows indicate the flow direction.

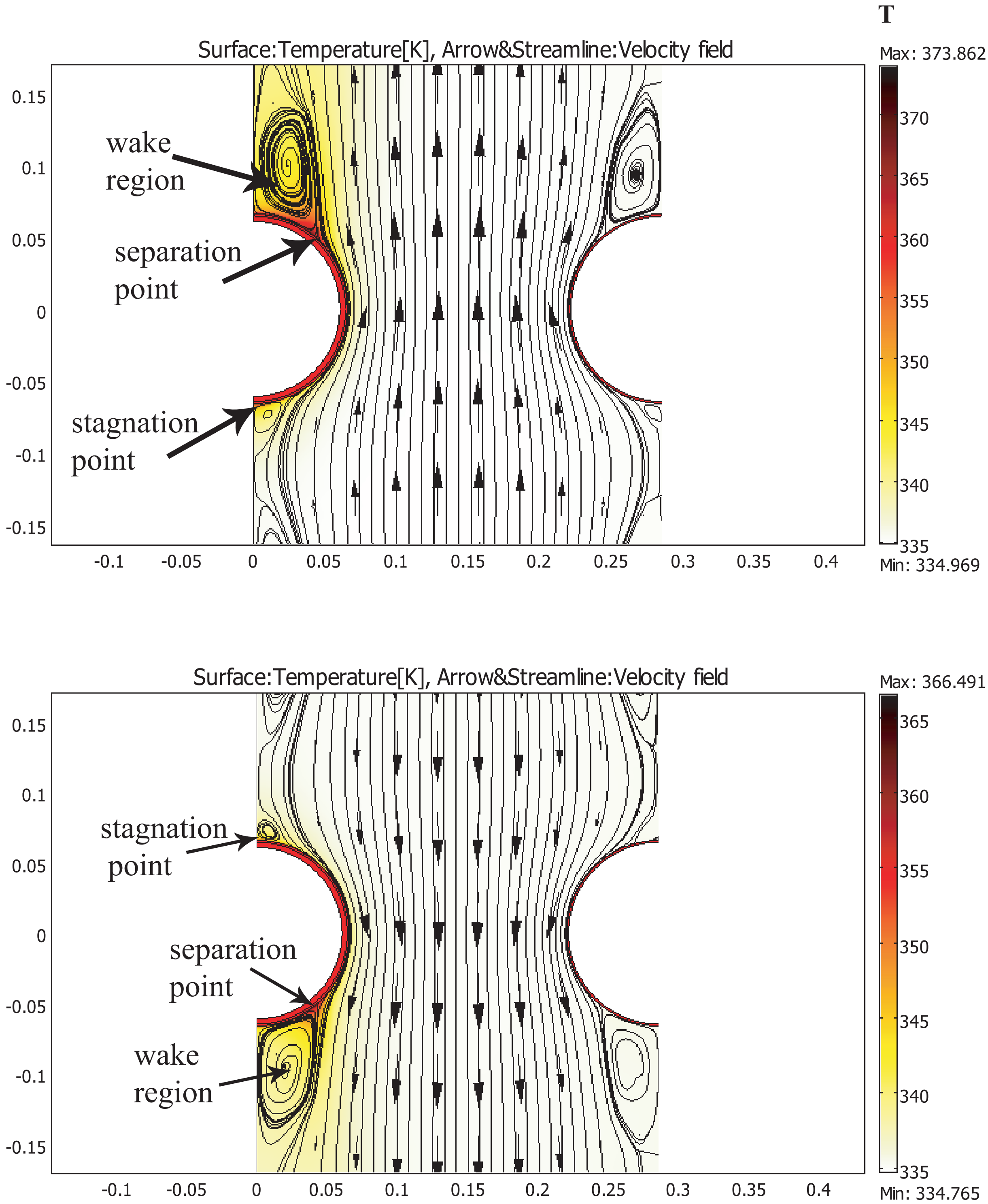

Figure 6. Velocity field around the CT for upward and downward flows

Figure 7 shows the velocity versus arc-length on the surface of the central CT after contact as percentage of the inflow velocity to the domain for upward and downward flows. The velocities in x and y direction are plotted separately and it is evident that the velocity in both directions is zero at the stagnation region ($L_s = [0 - 0.02]$ for upward flow and $L_s = [0.19 - 0.21]$ for downward flow) and this indicates that if boiling occurs, accumulation of vapor bubbles may produce a stable vapor film at this region which will reduce the local heat transfer coefficient. This can cause overheating of the CT surface and affect channel integrity if the vapor film extends around the tube. As a sensitivity analysis, different cases have been analyzed with different subcoolings and similar behavior was observed.

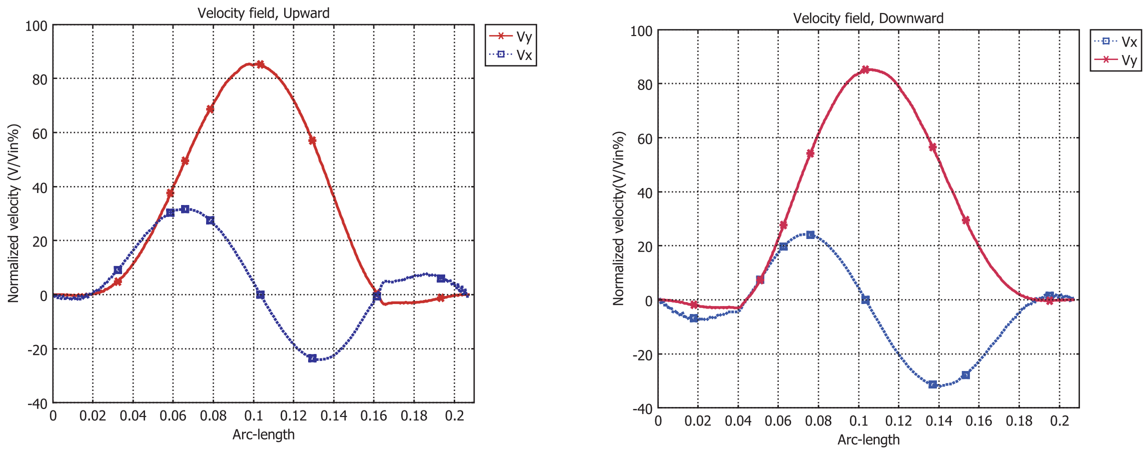

(a) **(b)**

Figure 7. Velocity field around the CT for a) upward and b) downward flows

Temperature distribution around the central CT is shown in Figure 8 for different subcoolings. Maximum temperature in the fluid is considered to be less than saturation. For each subcooling starting at the stagnation point, temperature decreases with increasing arc-length due to increase in velocity and heat transfer coefficient. However by developing the laminar boundary layer on the CT surface, the heat transfer coefficient decreases and temperature increases to its maximum value considered in this model. Eventually, separation occurs at $L = 0.16$ and fluid temperature declines due to the increase in heat transfer coefficient as a result of the considerable mixing associated with the wake region. However, as can be observed in the Figure8 the variations in local fluid temperature become smaller as subcooling reduces. Qualitatively, this indicates a greater tendency for vapor film to extend around the CT surface as subcooling decreases.

Density variations are shown in Figure 9. As the fluid heats up the density decreases and the velocity slightly increases. Thus, the boundary layer decreases and the local heat transfer coefficient should become larger. Neglecting the density variations in the model results in underestimation of the cooling/heating power. This points out the importance of taking density variations into account.

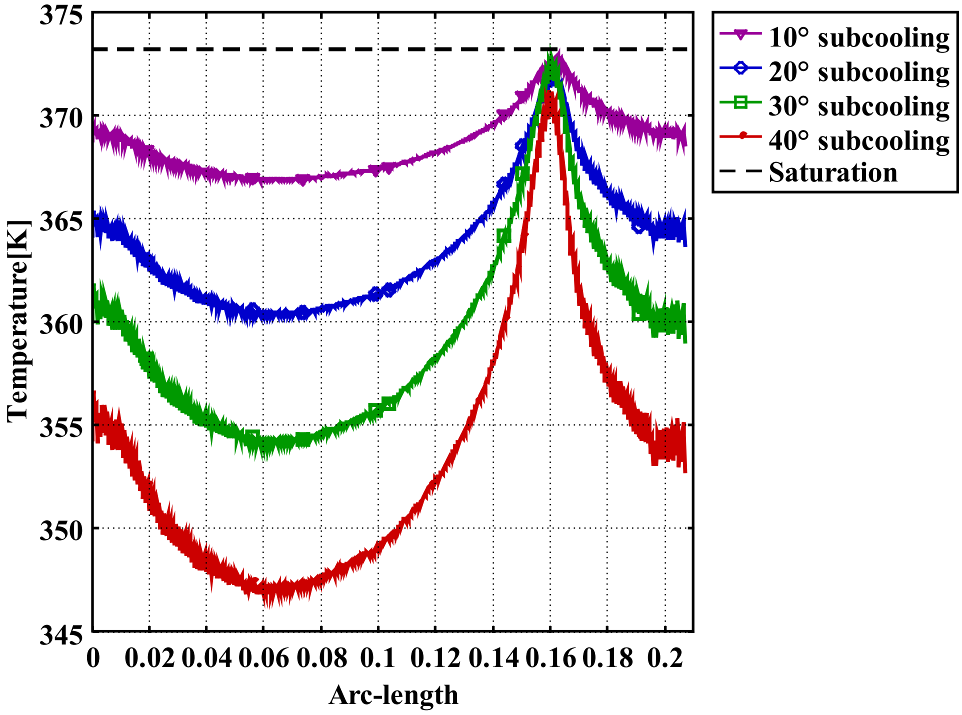

Figure 8. Local temperature around CT

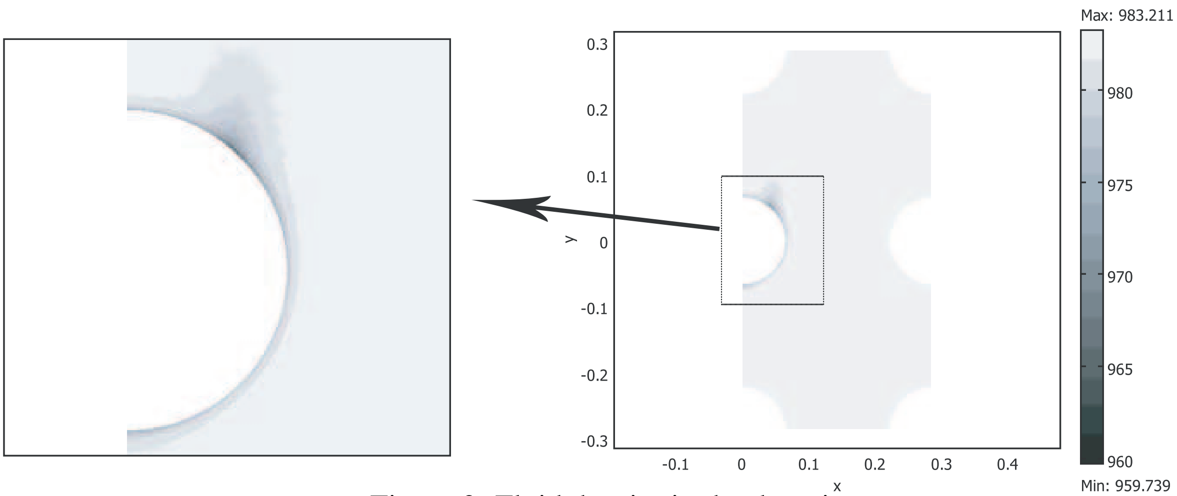

Figure 9. Fluid density in the domain

4. CONCLUSION

Flow field and temperature distribution around the calandria tube of a CANDU reactor fuel channel following PT/CT contact have been predicted. Buoyancy forces due to density variations has been taken into account and the fluid is considered to be single phase. Velocity, pressure and temperature profile around the cylinder are indicated. The model clearly indicates the wake region behind the cylinder. It also shows the stagnation region on the cylinder at which the velocity is zero and it can be concluded that the stagnated flow can result to accumulation of the bubbles and consequent stable vapor film generation at this region. The predicted local temperature variations with subcooling illustrates a greater tendency for vapor film to extend around the CT surface at low subcooling. Further simulation is being performed to investigate the behavior of bubble generation and thermal-hydraulic conditions in order to demonstrate the film boiling phenomena.

ACKNOWLEDGMENTS

The financial support of the Natural Science and Engineering Research Council (NSERC) and the University Network of Excellence in Nuclear Engineering (UNENE) is gratefully acknowledged.

REFERENCES

1. Churl Yoon, Boo Wook Rhee and Byung-Joo Min,“Development and Validation of the 3-D Computational Fluid Dynamics Model for CANDU-6 Moderator Temperature Predictions”, *Nuclear Technology*, v148, n3, p259-267, (2004).

2. Churl Yoon, Boo Wook Rhee, Hyoung Tae KIM, Joo Hwan PARK and Byung-Joo Min,“Moderator Analysis of Wolsong Units 2/3/4 for the 35% Reactor Inleat Header Break with a Loss of Emergency Core Cooling System”, *Journal of Nuclear Science and Technology*, v43, n5, p505-513, (2006).

3. Churl Yoon and Joo Hwan Park,“Development of a CFD model for the CANDU-6 Moderator Analysis using a Coupled Solver”, *Annals of Nuclear Energy*, v35, p1041-1049, (2007).

4. COMSOL Chemical Engineering Module User’s Guide, http://www.comsol.com, (2008).

5. D.C. Wilcox, “Turbulence Modeling for CFD”, DCW Industries Inc., (1998).

6. F. Incropera and D.DeWitt, “Introduction to Heat Transfer”, 2nd ed., (1990).

7. M. Holmgren, “XSteam for MATLAB, Thermodynamic Properties of Water and Steam”, http://www.mathworks.com, (2007).

8. G. Austman, J. Szymanski, M. Garceau and W.I. Midvidy, “Measuring Moderator Temperature in a CANDU Reactor”, 6^{th} *Annual Conference of CNS, Ottawa, Canada*, (1985).

9. H.F. Khartabil, W.W. Inch, J.K. Szymanski, D. Novog, V. Tavasoli and J. Mackinnon, "Three Dimentional Moderator Circulation Experimental Program for Validation of CFD code MODTURC-CLAS", 21^{st} *CNS Nuclear Simulation Symposium, Ottawa, Canada*, (2000).

10. J.C. Luxat, "Thermalhydraulic Aspects of Progression to Severe Accidents in CANDU Reactors", 12^{th} *International Topical Meeting on Nuclear Reactor Thermalhydraulics (NURETH-12), Pennsylvania, U.S.A.*, (2007).

11. J.K. Szymanski, K.C. Garceau and W.I. Midvidy, "Numerical Modeling of Three-Dimentional Turbulent Moderator Flow in Calandria", *Canadian Nuclear Society/American Nuclear Society International Conference on Numerical Methods in Nuclear Engineering*, v2, p970-84, (1983).

12. K.R. Mayoh, "A Compendium of Material Properties for Zirconium Alloys", COG-96-101, (1997).

13. Manwoong Kim, Seon-Oh Yu and Hho-Jung Kim,"Analysis on Fluid Flow and Heat Transfer inside Calandria vessel of CANDU-6 using CFD", *Nuclear Engineering and Design*, v236, n11, p1155-64, (2005).

14. O.C. Zienkiewicz and R.L. Taylor,"The Finite Element Method", 4th ed., v2, (1989).

15. R.G. Huget, J.K. Szymanski and W.I. Midvidy, "Status of Physical and Numerical Modelling of CANDU moderator circulation", *Proceedings of* 10^{th} *Annual Conference of Canadian Nuclear Society, Ottawa, Canada*, (1989).

16. R.G. Huget, J.K. Szymanski and W.I. Midvidy, "Experimental and Numerical Modelling of Combined Forced and Free Convection in a Complex Geometry with Internal Heat Generation", *Proceedings of* 9^{th} *International Heat Transfer Conference, Jeursalem, Israel*, (1990).

17. W.M. Kays, "Turbulent Prandtl Number. Where Are We?" *Journal of Heat Transfer*, v116, p284-295, (1994).